

# Study of the process $e^+e^- \rightarrow K^+K^-\pi^0$ in the center-of-mass energy range 1.2–2 GeV with the CMD-3 detector

Andrei Erofeev<sup>1,2,\*</sup> and CMD-3 Collaboration<sup>1</sup>

<sup>1</sup>Budker Institute of Nuclear Physics SB RAS, Novosibirsk 630090

<sup>2</sup>Novosibirsk State University, Novosibirsk 630090

**Abstract.** The process  $e^+e^- \rightarrow K^+K^-\pi^0$  has been studied at a center-of-mass energy range from 1.2 to 2 GeV using a  $80.6\text{ pb}^{-1}$  data sample collected with the CMD-3 detector at the electron-positron collider VEPP-2000. The preliminary results of the cross-section measurement are presented.

## 1 Introduction

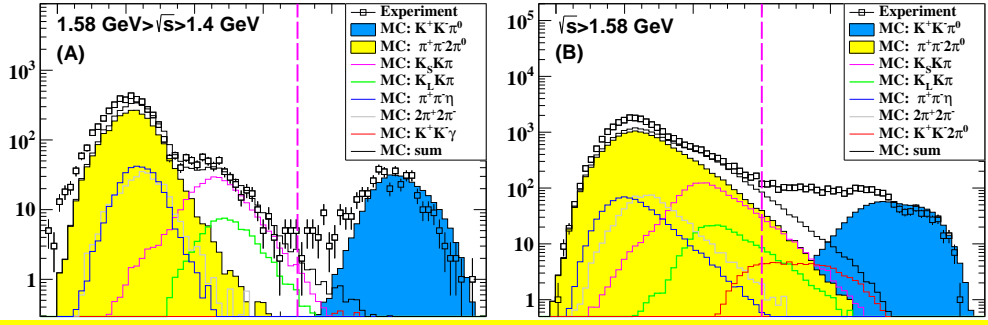
The process  $e^+e^- \rightarrow K^+K^-\pi^0$  has been studied up to now with low statistical accuracy by the BABAR and DM2 experiments. **There are no references to babar and dm2 papers** for precise calculation of the hadronic contribution to the muon  $g-2$ . A detailed study of the production dynamics will improve theoretical models of the light hadron production.

The general-purpose detector CMD-3 has been described in detail elsewhere [1]. The tracking system consists of the cylindrical drift chamber (DC) and double-layer multi-wire proportional Z-chamber with both subsystems installed inside a thin superconducting solenoid with 1.0-1.3 T magnetic field. Both subsystems are used to generate a trigger signal. The DC contains 1218 hexagonal cells and performs a measurement of the momentum, polar ( $\theta$ ) and azimuth ( $\phi$ ) angles of the charged particles. The barrel electromagnetic calorimeters placed outside the solenoid are based on liquid xenon (LXe) and CsI crystals with a thickness of  $5.4 X_0$  and  $8.1 X_0$ , respectively. The endcap calorimeter is made of BGO scintillation crystals with a thickness of  $13.4 X_0$ .

## 2 Data analysis

The signal events identification technique involves the detection of two charged kaons and two photons formed as a result of  $\pi^0$  decay. So, all candidate events are characterized by two tracks with zero total charge and at least two photons. We require the tracks to originate from the beam interaction region in a 10 cm neighborhood along the beam axis with impact parameter no **more than 0.4 cm. why 0.4 cm? not 0.2, ex.** ed by noncollinear track selection condition expressed by inequalities  $||\varphi_1 - \varphi_2| - \pi| > 0.15\text{ rad}$  and  $|\theta_1 + \theta_2 - \pi| > 0.25\text{ rad}$ , forming a rather effective approach to rejection of cosmic rays and beam background events. The tracks are also required to pass over the central part of the DC for the best agreement between experiment and simulation:  $|\theta - \pi/2| < 0.8\text{ rad}$ .

\*e-mail: andrikola@yandex.ru



I have not found the description of the figure in text. The explanation in caption should be

**Figure 1.** Separation of the signal and background events in the range of medium energies (A) and high energies (B). The legend indicates the different Monte Carlo (MC) background processes and the sum of all backgrounds (MC: sum). The x-axis represents the BDT parameter, and the y-axis represents the event count. The experimental data is shown as black squares, and the various MC backgrounds are shown as colored lines. A vertical dashed pink line is drawn at approximately 10<sup>2.5</sup> on the x-axis.

the main background processes expected from the simulation. Separation of the signal and background

Is the MC sum a sum of backgrounds? Please, demonstrate a comparison of data and the sum

Now we turn to higher-level selections, the main purpose of which is to separate the signal process events from the events of other possible channels of  $e^+e^-$  annihilation. To avoid cumbersome symbolic expressions, let us denote the energy of a particle with mass  $m$  and 3-momentum  $\mathbf{p}$  by a symbol  $\mathcal{E}(\mathbf{p}, m)$ . Then the track momenta  $\mathbf{p}_1$  and  $\mathbf{p}_2$  must satisfy an inequality  $\mathcal{E}(\mathbf{p}_1 - \mathbf{p}_2, m_\pi) \leq \sqrt{s} - \mathcal{E}(\mathbf{p}_1, m_K) - \mathcal{E}(\mathbf{p}_2, m_K) \leq \mathcal{E}(\mathbf{p}_1 + \mathbf{p}_2, m_\pi)$  resulting from the kinematics of the process being studied. We impose this restriction on the measured track momenta. Event selection is also performed on the total momentum  $P = |\mathbf{p}_1 + \mathbf{p}_2 + \mathbf{k}_1 + \mathbf{k}_2|$  and the total energy difference  $\Delta E = |\sqrt{s} - \mathcal{E}(\mathbf{p}_1, m_K) - \mathcal{E}(\mathbf{p}_2, m_K) - |\mathbf{k}_1| - |\mathbf{k}_2||$ , where  $\mathbf{p}$  and  $\mathbf{k}$  denote the 3-momenta of the track and the photon, respectively. We require  $P < 0.16$  GeV/c and  $\Delta E < 0.18$  GeV.

We perform a 4C-kinematic fit (KF) for every possible pair of detected photons with energy more than 20 MeV in an event requiring the energy-momentum conservation without applying a mass constraint. The fit reconstructs the momenta and angles of the selected tracks and photons. The photon pair producing the lowest  $\chi^2$  is retained if the reconstructed energies of both quanta  $E_\gamma > 40$  MeV.

An essential part of background suppression is the selection of high-momentum tracks. The low momentum tracks ( $p < 500$  MeV/c) of pions and ... from a process  $e^+e^- \rightarrow \pi^+\pi^-\pi^0\pi^0$ . The tracks of pions and kaons are well separated by ionization losses in the DC unless the momenta of these particles are higher than 500 MeV/c. To suppress these parasitic processes at high  $\sqrt{s}$  we have to use kinematics additionally.

A significant background contribution, as simulation shows, is also represented by the processes of  $e^+e^-$  annihilation into final states:  $K^+K^-\pi^0\pi^0$ ,  $K_S^0K\pi$ ,  $K_L^0K\pi$  and  $K^+K^-\gamma$ . The events of the former are well separated at high energies by the squared recoil mass of the tracks  $M_{rec}^2 = (\sqrt{s} - |\mathbf{p}_1| - |\mathbf{p}_2|)^2 - (\mathbf{p}_1 + \mathbf{p}_2)^2$ , where  $\mathbf{p}_1$  and  $\mathbf{p}_2$  are track momenta before kinematic reconstruction.

For further background suppression, please, let me to see the distributions of parameters used in BDT. method. In accordance with stated above we accepted as BDT arguments the ionization losses  $dE/dx$  of the tracks in the DC, the track momenta after kinematic reconstruction, the momenta and angles  $\theta$  of the photons after KF and the parameter  $M_{rec}^2$ . To train and test the classifier we use GEANT4 [2] based Monte Carlo simulation of the signal and all mentioned background processes. Shown in Figure 1 are distributions of the BDT parameter for experimental and simulated data. Due to the overlapping of the  $dE/dx$  distributions of

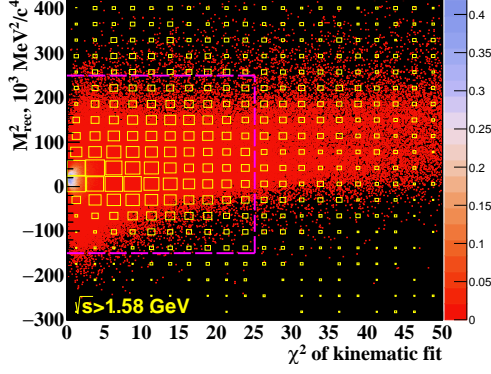


**Figure 2.** Squared recoil mass  $M_{rec}^2$  vs  $\chi^2$  of kinematic reconstruction for the simulation (scatter-plot) and the experimental data (box diagram). The dashed lines designate cut lines.

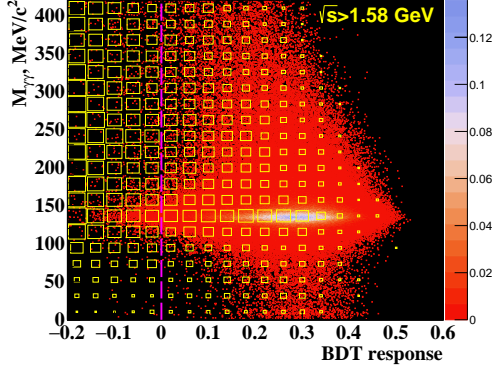


**Figure 3.** The photon pair invariant mass  $M_{\gamma\gamma}$  vs BDT response for the simulation (scatter-plot) and the experimental data (box diagram). The dashed line designates cut line.

the dashed lines correspond to applied criterion

different particles with the track momenta over 500 MeV, the background suppression quality drops significantly at high energies as also can be seen from the Figure 1. In order to improve this situation we limit the possible values of the KF  $\chi^2$  and  $M_{rec}^2$  as shown in Figure 2 by the dashed lines. The resulting distribution of the invariant photon mass  $M_{\gamma\gamma}$  vs the BDT response is shown in the Figure 3 where we can see the presence of the signal. However after all the selections are applied, the number of background events is comparable to the yield of the studied process at high  $\sqrt{s}$ .

The signal yield at each energy point is determined from the fit of the photon pair invariant mass distribution for events that satisfy all mentioned above selection criteria. More specifically, we proceed as follows. The energy range is divided into several intervals. The invariant mass spectrum of selected experimental events from each energy interval is approximated by a function  $F(x) = p_0 F_{2K\pi}(x) + p_1 F_{4\pi}(x) + p_2 + p_3 x + p_4 x^2 \equiv p_0 F_{2K\pi}(x) + F_{bg}(x)$ , where  $p_i$  are parameters of approximation,  $F_{2K\pi}$  and  $F_{4\pi}$  denote functions describing the contributions of the signal and the process  $e^+e^- \rightarrow \pi^+\pi^-\pi^0\pi^0$ , which are determined from the simulation. The  $M_{\gamma\gamma}$  spectrum at each energy point is fitted by a function  $F(x) = q_0 F_{2K\pi}(x) + q_1 F_{bg}(x)$ , where  $F_{2K\pi}$  is taken from the simulation for given  $\sqrt{s}$  and  $q_i$  are new fit parameters. The signal appear to be absent at  $\sqrt{s} < 1.38$  GeV. The total signal yield is estimated to be  $2824 \pm 54$  (Figure 4).

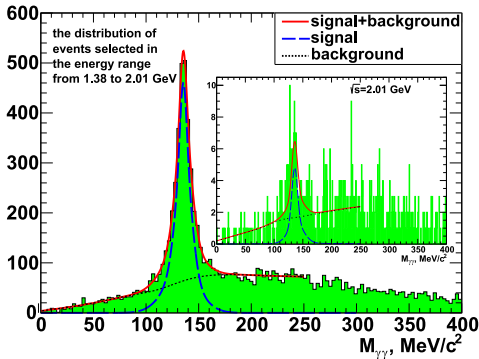


**Figure 4.** The approximation of the photon pair invariant mass spectrum of experimental events in  $\sqrt{s}$  range from 1.38 to 2.01 GeV. Also shown is the approximation for one energy point (in this case  $\sqrt{s} = 2.01$  GeV).

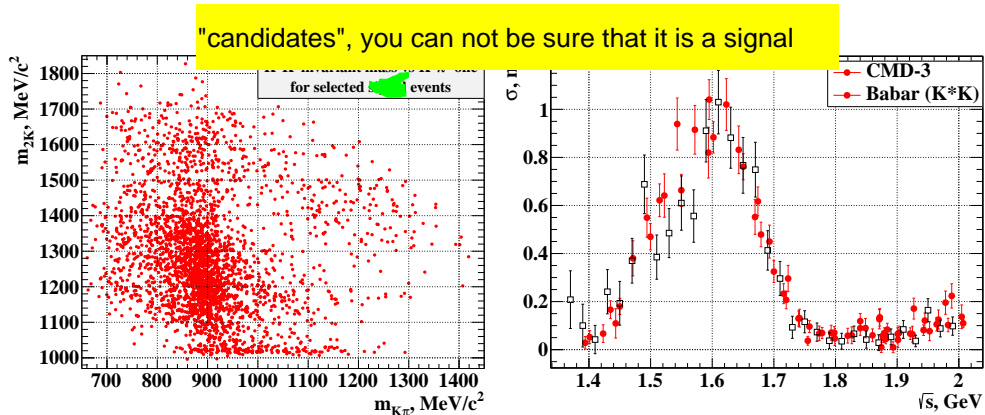


**Figure 5.** The Dalitz plot distribution for the signal events selected in the energy range from 1.38 to 2.01 GeV.

**Figure 6.** Cross section of  $e^+e^- \rightarrow K^+K^-\pi^0$  process in comparison with the previous BABAR measurement.

## 3. Results

The spectrum in Fig. 5 ...

Shown in Figure 5 is the Dalitz plot distribution in coordinates of the  $K^+\pi^0$  and  $K^+K^-$  invariant masses for signal events selected. A small contribution of the  $\phi\pi^0$  intermediate state is evident.

The Born cross section at the  $i$ -th energy point  $s_i$  is determined by the standard formula  $\sigma_B(s_i) = N_i/(\epsilon_i L_i (1 + \delta_{rc,i}))$ , where  $N_i$ ,  $\epsilon_i$ ,  $L_i$  and  $\delta_{rc,i}$  denote the number of signal events, detection efficiency, luminosity and radiation correction, respectively. The detection efficiency was determined from MC simulation of the signal process according to the  $e^+e^- \rightarrow K^*K$  model as this intermediate mechanism is known to dominate the process. The result is shown in Figure 6 in comparison with the cross section previously measured by BABAR [3] for the  $K^*K$  intermediate state.

The measured values of cross section is shown in Fig. 6 in comparison with BABAR result [3].

The presented results are preliminary. Event selection algorithm has been developed and the

Preliminary results in the study of .... is presented here.

increase measurement accuracy.

All authors would like to thank the Russian Foundation for Basic Research (RFBR), grant 17-52-50064.

## References

- [1] B. I. Khazin et al. (CMD-3 collaboration), Nucl. Phys. B Proc. Suppl. **376**, 181-182 (2008).
- [2] S. Agostinelli et al. (GEANT4 Collaboration), Nucl. Instrum. Methods Phys. Res. A **506**, 250 (2003).
- [3] B. Aubert et al. (BABAR collaboration), Phys. Rev. D **77** 092002 (2008).